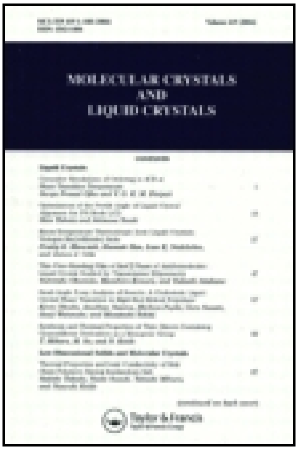

Molecular Crystals and Liquid Crystals
Publication details, including instructions for authors and subscription information:
http://www.tandfonline.com/loi/gmcl20

Laterally Brominated Symmetric Liquid Crystal Trimers with (S)-(-)-2-Methylbutyl-4′-(4″-phenyl)benzoate Exhibiting N* and Blue Phases

Guan-Yeow Yeap [a] , Tiang-Chuan Hng [a] , Masato M. Ito [b] , Wan Ahmad Kamil Mahmood [a] , Daisuke Takeuchi [c] & Kohtaro Osakada [c]

[a] Liquid Crystal Research Laboratory, School of Chemical Sciences, University Sains Malaysia, Minden, Penang, Malaysia

[b] Department of Environmental Engineering for Symbiosis, Faculty of Engineering, Soka University, Hachioji, Tokyo, Japan

[c] Chemical Resources Laboratory, Tokyo Institute of Technology, Midori-ku, Yokohama, Japan

Version of record first published: 17 Dec 2009

To cite this article: Guan-Yeow Yeap, Tiang-Chuan Hng, Masato M. Ito, Wan Ahmad Kamil Mahmood, Daisuke Takeuchi & Kohtaro Osakada (2009): Laterally Brominated Symmetric Liquid Crystal Trimers with (S)-(-)-2-Methylbutyl-4′-(4″-phenyl)benzoate Exhibiting N* and Blue Phases, Molecular Crystals and Liquid Crystals, 515:1, 215-229

To link to this article: http://dx.doi.org/10.1080/15421400902987594

Mol. Cryst. Liq. Cryst., Vol. 515, pp. 215–229, 2009
Copyright © Taylor & Francis Group, LLC
ISSN: 1542-1406 print/1563-5287 online
DOI: 10.1080/15421400902987594

Laterally Brominated Symmetric Liquid Crystal Trimers with (S)-(-)-2-Methylbutyl-4′-(4″-phenyl)benzoate Exhibiting N* and Blue Phases

Guan-Yeow Yeap[1], Tiang-Chuan Hng[1], Masato M. Ito[2], Wan Ahmad Kamil Mahmood[1], Daisuke Takeuchi[3], and Kohtaro Osakada[3]
[1]Liquid Crystal Research Laboratory, School of Chemical Sciences, University Sains Malaysia, Minden, Penang, Malaysia
[2]Department of Environmental Engineering for Symbiosis, Faculty of Engineering, Soka University, Hachioji, Tokyo, Japan
[3]Chemical Resources Laboratory, Tokyo Institute of Technology, Midori-ku, Yokohama, Japan

The series of eight symmetric trimers, 4,4′-bis{ω-[2-methylbutyl-4′-(4″-phenyl) benzoateoxy]-3-bromo-4-alkyloxybenzylidene}-1,4-phenylenediamines has been synthesized and characterized. Except pentyl and undecyl homologues, the seven-ring chiral trimers exhibit the enantiotropic N phase. In addition to the N* phase, the odd trimers with heptyl and nonyl spacers also exhibit the blue phase with platelet texture. The nematogenic properties of the trimers are attributed to the presence of two lateral bulky bromine atoms in the central mesogenic core. The suppression of mesophase thermal stability is largely due to the increase in molecular breadth at positions the bromine atoms are attached, which results in weaker overall lateral intermolecular attraction. The thermal properties of the trimers are also compared to those of the earlier reported analogous trimers that do not possess any lateral substituents in the mesogenic cores.*

Keywords: blue phase; bromine atom; lateral; N* phase; symmetric trimer

1. INTRODUCTION

Liquid crystal oligomers have often been regarded as a model for the semiflexible main-chain liquid crystalline polymers that are known to possess great application value [1]. In order to understand

Address correspondence to Guan-Yeow Yeap, Liquid Crystal Research Laboratory, School of Chemical Sciences, University Sains Malaysia, 11800 Minden, Penang, Malaysia. E-mail: gyyeap@usm.my or gyyeap_liqcryst_usm@yahoo.com

further the physical and chemical properties of the polymers, the research in liquid crystal oligomers has then been carried out extensively only to discover that these materials also exhibit unique liquid crystal properties that are not observed for conventional liquid crystals [1–4].

Liquid crystal dimers, with two mesogenic groups connected by one flexible spacer are the shortest of all members of oligomer. Various mesogenic groups, such as the heterocyclic benzoxazole, have been introduced into the system of dimers [5]. The significant findings on the dimers have prompted researchers to also synthesize its longer counterpart with three mesogenic groups connected by two spacers which are known as the trimers or trimesogens [6]. The trimers are important in the research of liquid crystal oligomers as differences in their mesomorphic properties as compared to those of the dimers have been observed. One of the differences is the greater magnitude alternation exhibited by the nematic–isotropic transition temperatures of the trimers as compared to the dimers [1].

A series of chiral symmetric trimers we reported recently exhibit high mesophase thermal stability. For instance, the trimer with two C_6H_{12} spacers possesses clearing temperature of 266.0°C [7]. Such thermal properties of the trimers are mainly attributed to the long calamitic molecular structure and the presence of seven aromatic rings which favours strong intermolecular attraction. As the continuation of our effort to further investigate the properties of the seven-ring liquid crystal trimers mentioned above, we present another novel series of the homologous trimers incorporating two lateral bromine atoms in the benzylidene-1,4-phenylenediamine central mesogenic group. Previous studies have shown that the mesomorphic properties of laterally substituted liquid crystals are dependent on the type and size of the substituents as well as other factors such as polarizability and/or polarity [8,9]. Mesogens with relatively large lateral substituents such as the CH_3 or OCH_3 groups exhibit lower phase transition temperatures and lower-ordered mesophases as the result of reduced lateral intermolecular attraction [10,11].

2. EXPERIMENTAL

The series of α,ω-dibromoalkanes, (S)-(-)-2-methyl-1-butanol and 4-(4-hydroxyphenyl)benzoic acid were purchased from TCI, Japan. The 3-bromo-4-hydroxybenzaldehyde was obtained from Sigma-Aldrich, USA whilst *p*-phenylenediamine was made available by Acros Organics, Belgium. The chemicals were used directly from the bottles without further purification.

2.1. Synthesis of Materials

The preparative pathway towards obtaining title compounds **4a–4h** is shown in Scheme 1. Compound **1** was synthesized via condensation reaction in similar manner as reported elsewhere [5]. Compounds **2a–2h** resulted from the Williamson ether synthetic reactions between compound **1** and various α,ω-dibromoalkanes ranging from $C_5H_{10}Br_2$ to $C_{12}H_{24}Br_2$. The Fischer acid-catalyzed esterification between 4-(4-hydroxyphenyl)benzoic acid and (S)-(-)-2-methyl-1-butanol gave the ester intermediary compound **3**. The freshly prepared compounds **2a–2h** were subsequently reacted with compound **3** via Williamson method to yield the desired compounds **4a–4h**.

2.1.1. *Synthesis of Compound* 4a

In a round-bottom flask, compound **3**, potassium carbonate anhydrous, and catalytic amount of potassium iodide were mixed and heated in 30 mL acetone. Compound **2a** was dissolved in 20 mL N,N-dimethylformamide and then added dropwise to the stirring acetone solution. The resulting mixture was subsequently refluxed for 18 h before being left at room temperature for acetone to evaporate off. Upon addition of water, the resulting precipitate was filtered off under

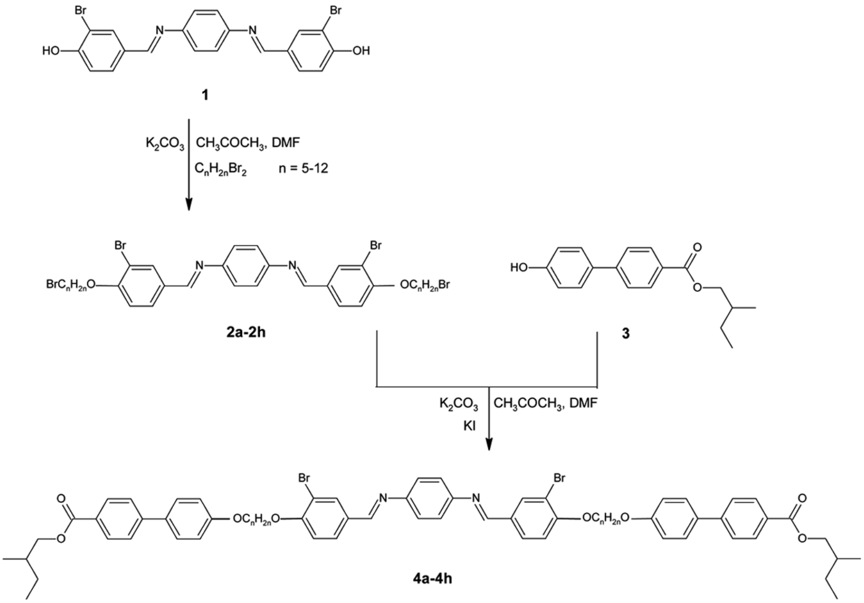

SCHEME 1 The synthetic pathway towards formation of compounds **4a–4h**.

reduced pressure and dried. The precipitate was recrystallized from ethyl acetate to yield the desired yellow powder. Yield 70%. Elemental analysis (%): found, C 67.25, H 6.00, N 2.39; calculated ($C_{66}H_{70}N_2O_8Br_2$), C 67.23, H 5.98, N 2.38. IR (KBr) ν/cm^{-1}, 2959–2872 (C−H alkyl), 1712 (C=O ester), 1617–1602 (C=N), 1268 (O-CH$_2$). ^{1}H-NMR (CDCl$_3$) δ/ppm, 0.99 (t, 6 H, CH$_3$), 1.06 (d, 6 H, CH$_3$), 1.35 (m, 2H, CH$_2$), 1.55–2.02 (m, 16 H, CH, and CH$_2$), 4.09–4.17 (2 t, 8 H, OCH$_2$), 4.14–4.27 (2 dd, 4 H, OCH$_2$), 6.99 (d, 2 H, Ar), 7.03 (d, 4 H, Ar), 7.27 (s, 4 H, Ar), 7.60 (d, 4 H, Ar), 7.65 (d, 4 H, Ar), 7.78 (dd, 2 H, Ar), 8.09 (d, 4 H, Ar), 8.19 (d, 2 H, Ar), 8.40 (s, 2 H, CH=N).

2.1.2. *Synthesis of Compound* 4b

Yield 60%. Elemental analysis (%): found, C 67.67, H 6.21, N 2.32; calculated ($C_{68}H_{74}N_2O_8Br_2$), C 67.66, H 6.18, N 2.32. IR (KBr) ν/cm^{-1}, 2961–2874 (C−H alkyl), 1711 (C=O ester), 1618–1603 (C=N), 1269 (O−CH$_2$). ^{1}H-NMR (CDCl$_3$) δ/ppm, 0.99 (t, 6 H, CH$_3$), 1.06 (d, 6 H, CH$_3$), 1.35 (m, 2 H, CH$_2$), 1.57–1.95 (m, 20 H, CH, and CH$_2$), 4.06–4.14 (2 t, 8 H, OCH$_2$), 4.14–4.27 (2 dd, 4 H, OCH$_2$), 6.98 (d, 2 H, Ar), 7.00 (d, 4 H, Ar), 7.27 (s, 4 H, Ar), 7.57 (d, 4 H, Ar), 7.66 (d, 4 H, Ar), 7.77 (dd, 2 H, Ar), 8.09 (d, 4 H, Ar), 8.19 (d, 2 H, Ar), 8.40 (s, 2 H, CH=N).

2.1.3. *Synthesis of Compound* 4c

Yield 65%. Elemental analysis (%): found, C 68.09, H 6.38, N 2.28; calculated ($C_{70}H_{78}N_2O_8Br_2$), C 68.07, H 6.37, N 2.27. IR (KBr) ν/cm^{-1}, 2934–2856 (C−H alkyl), 1709 (C=O ester), 1615–1593 (C=N), 1268 (O−CH$_2$). ^{1}H-NMR (CDCl$_3$) δ/ppm, 0.99 (t, 6 H, CH$_3$), 1.04 (d, 6 H, CH$_3$), 1.35 (m, 2 H, CH$_2$), 1.52–1.95 (m, 24 H, CH, and CH$_2$), 4.05–4.13 (2 t, 8 H, OCH$_2$), 4.14–4.26 (2 dd, 4 H, OCH$_2$), 6.98 (d, 2 H, Ar), 7.02 (d, 4 H, Ar), 7.27 (s, 4 H, Ar), 7.60 (d, 4 H, Ar), 7.65 (d, 4 H, Ar), 7.77 (dd, 2 H, Ar), 8.12 (d, 4 H, Ar), 8.19 (d, 2 H, Ar), 8.40 (s, 2 H, CH=N).

2.1.4. *Synthesis of Compound* 4d

Yield 59%. Elemental analysis (%): found, C 68.47, H 6.56, N 2.24; calculated ($C_{72}H_{82}N_2O_8Br_2$), C 68.46, H 6.54, N 2.22. IR (KBr) ν/cm^{-1}, 2933–2855 (C−H alkyl), 1709 (C=O ester), 1617–1594 (C=N), 1268 (O−CH$_2$). ^{1}H-NMR (CDCl$_3$) δ/ppm, 0.99 (t, 6 H, CH$_3$), 1.06 (d, 6 H, CH$_3$), 1.35 (m, 2 H, CH$_2$), 1.46–1.93 (m, 28 H, CH, and CH$_2$), 4.03–4.12 (2 t, 8 H, OCH$_2$), 4.15–4.27 (2 dd, 4 H, OCH$_2$), 6.98 (d, 2 H, Ar), 7.00 (d, 4 H, Ar), 7.29 (s, 4 H, Ar), 7.58 (d, 4 H, Ar), 7.65 (d, 4 H, Ar), 7.78 (dd, 2 H, Ar), 8.10 (d, 4 H, Ar), 8.19 (d, 2 H, Ar), 8.40 (s, 2 H, CH=N).

2.1.5. ***Synthesis of Compound* 4e**

Yield 70%. Elemental analysis (%): found, C 68.85, H 6.74, N 2.18; calculated ($C_{74}H_{86}N_2O_8Br_2$), C 68.83, H 6.71, N 2.17. IR (KBr) ν/cm^{-1}, 2934–2853 (C−H alkyl), 1713 (C=O ester), 1616–1592 (C=N), 1267 (O−CH$_2$). ^{1}H-NMR (CDCl$_3$) δ/ppm, 0.99 (t, 6 H, CH$_3$), 1.06 (d, 6 H, CH$_3$), 1.35 (m, 2 H, CH$_2$), 1.42–1.92 (m, 32 H, CH, and CH$_2$), 4.03–4.12 (2 t, 8 H, OCH$_2$), 4.14–4.27 (2 dd, 4 H, OCH$_2$), 6.98 (d, 2 H, Ar), 7.02 (d, 4 H, Ar), 7.29 (s, 4 H, Ar), 7.57 (d, 4 H, Ar), 7.63 (d, 4 H, Ar), 7.77 (dd, 2 H, Ar), 8.09 (d, 4 H, Ar), 8.18 (d, 2 H, Ar), 8.40 (s, 2 H, CH=N).

2.1.6. ***Synthesis of Compound* 4f**

Yield 71%. Elemental analysis (%): found, C 69.19, H 6.90, N 2.13; calculated ($C_{76}H_{90}N_2O_8Br_2$), C 69.19, H 6.88, N 2.12. IR (KBr) ν/cm^{-1}, 2927–2853 (C−H alkyl), 1709 (C=O ester), 1616–1592 (C=N), 1268 (O−CH$_2$). ^{1}H-NMR (CDCl$_3$) δ/ppm, 0.98 (t, 6 H, CH$_3$), 1.06 (d, 6 H, CH$_3$), 1.35–1.92 (m, 38 H, CH, and CH$_2$), 4.03–4.12 (2 t, 8 H, OCH$_2$), 4.14–4.28 (2 dd, 4 H, OCH$_2$), 6.98 (d, 2 H, Ar), 7.02 (d, 4 H, Ar), 7.27 (s, 4 H, Ar), 7.56 (d, 4 H, Ar), 7.65 (d, 4 H, Ar), 7.76 (dd, 2 H, Ar), 8.08 (d, 4 H, Ar), 8.18 (d, 2 H, Ar), 8.40 (s, 2 H, CH=N).

2.1.7. ***Synthesis of Compound* 4g**

Yield 60%. Elemental analysis (%): found, C 69.55, H 7.04, N 2.08; calculated ($C_{78}H_{94}N_2O_8Br_2$), C 69.53, H 7.03, N 2.08. IR (KBr) ν/cm^{-1}, 2922–2852 (C−H alkyl), 1714 (C=O ester), 1616–1592 (C=N), 1267 (O−CH$_2$). ^{1}H-NMR (CDCl$_3$) δ/ppm, 0.99 (t, 6 H, CH$_3$), 1.06 (d, 6 H, CH$_3$), 1.35–1.91 (m, 42 H, CH, and CH$_2$), 4.02–4.11 (2 t, 8 H, OCH$_2$), 4.15–4.28 (2 dd, 4 H, OCH$_2$), 6.98 (d, 2 H, Ar), 7.02 (d, 4 H, Ar), 7.27 (s, 4 H, Ar), 7.56 (d, 4 H, Ar), 7.65 (d, 4 H, Ar), 7.76 (dd, 2 H, Ar), 8.09 (d, 4 H, Ar), 8.18 (d, 2 H, Ar), 8.39 (s, 2 H, CH=N).

2.1.8. ***Synthesis of Compound* 4h**

Yield 66%. Elemental analysis (%): found, C 69.87, H 7.21, N 2.05; calculated ($C_{80}H_{98}N_2O_8Br_2$), C 69.86, H 7.18, N 2.04. IR (KBr) ν/cm^{-1}, 2923–2852 (C−H alkyl), 1711 (C=O ester), 1601–1592 (C=N), 1273 (O−CH$_2$). ^{1}H-NMR (CDCl$_3$) δ/ppm, 0.99 (t, 6 H, CH$_3$), 1.06 (d, 6 H, CH$_3$), 1.33–1.89 (m, 46 H, CH, and CH$_2$), 4.03–4.11 (2 t, 8 H, OCH$_2$), 4.14–4.27 (2 dd, 4 H, OCH$_2$), 6.98 (d, 2 H, Ar), 7.02 (d, 4 H, Ar), 7.27 (s, 4 H, Ar), 7.57 (d, 4 H, Ar), 7.65 (d, 4 H, Ar), 7.77 (dd, 2 H, Ar), 8.09 (d, 4 H, Ar), 8.18 (d, 2 H, Ar), 8.40 (s, 2 H, CH=N).

2.2. Measurements

The molecular structures of the intermediary and title compounds were characterized by FT-IR and ^{1}H-NMR spectroscopy. The FT-IR spectroscopy was performed on a Perkin Elmer 2000 FT-IR spectrometer. The samples were dispersed homogenously in KBr powder and compressed into pellets. The spectra were recorded in the range of 4000–400 cm^{-1}. For ^{1}H-NMR spectroscopy, the sample was dissolved in 0.7 mL of $CDCl_3$ which contains 0.03 v/v% of TMS as internal standard and the analyses were carried out on a Bruker 400 MHz Ultrashield^{TM} spectrometer. CHN microanalyses were conducted on a Perkin Elmer 2400 LS Series CHNS/O analyzer. The mesophase textures were observed using a Carl Zeiss Axioskop 40 polarizing microscope with a Linkam LTS350 hot-stage of which the sample temperature was regulated by Linkam TMS94 temperature controller. The phase transition temperatures and associated enthalpies were determined by Seiko DSC6200 R calorimeter with the heating and cooling rate of ±5°C min^{-1} at Tokyo Institute of Technology, Japan.

3. RESULTS AND DISCUSSION

3.1. Odd–Even Effect

The phase transition temperatures and associated enthalpies of the title compounds **4a–4h** upon heating cycle are tabulated in Table 1. The dependence of phase transition temperatures of these homologues on the number of methylene units, n in the spacers is plotted in Fig. 1. Across the series, the melting temperatures show no regular dependence on the length of the spacer. For instance, the lowest melting point is recorded for compound **4c**, whilst the melting point for compound **4b** is only 3.2°C higher than that of compound **4g** even though **4g** has five methylene units per spacer more than **4b**. On the other hand, the commonly observed zigzag pattern or the odd-even effect in oligomers is observed for the clearing temperatures of compounds **4b–4h**. The even members possess higher clearing temperatures than the odd counterparts. As the series ascends towards the longer members, the N^*-I transition temperatures attenuates consistently. Such attenuation of nematic-isotropic temperatures has been observed in various homologous systems of liquid crystal oligomers, both chiral and achiral such as the non-symmetric dimers with 4-cyanobiphenyl mesogenic core [12]. It is important to mention that the N^* phase of compound **4g** is monotropic. A mesomorphic trend is, however, observable as the odd spacer length is increased from C_5H_{10} to $C_{11}H_{22}$, of which the lengthening of the spacer can also justify the monotropic

TABLE 1 Phase Transition Temperatures (°C), Associated Enthalpies ($kJmol^{-1}$), and Chiral Nematic–isotropic Entropy Changes of Compounds **4a**–**4h**. Only the Highest Melting Points are Reported. (● = enantiotropic phase, ○ = monotropic phase, Cr = crystal, N^* = chiral nematic, BP = blue phase, I = isotropic)

Compound	Cr		N^*		BP		I	$\Delta S_{N^*I}/R$
4a	●	137.4 (12.3)					●	–
4b	●	146.5 (4.0)	●	213.6 (1.5)			●	3.17
4c	●	116.3 (12.0)	●	140.5[a] (0.2)[a]	●	140.5[a] (0.2)[a]	●	0.49[b]
4d	●	120.7 (12.2)	●	190.0 (2.1)			●	4.53
4e	●	130.4 (14.9)	●	142.6[a] (0.2)[a]	●	142.6[a] (0.2)[a]	●	0.45[b]
4f	●	126.8 (9.0)	●	169.7 (1.6)			●	3.62
4g	●	143.3 (19.1)	○	138.0 (0.4)			●	–
4h	●	122.9 (13.3)	●	159.5 (1.9)			●	4.44

[a] The N^*-BP and BP-I respective transition temperatures and enthalpies are unresolved in the DSC thermograms.

[b] The $\Delta S_{N^*I}/R$ values for **4c** and **4e** are obtained from the unresolved N^*-BP and BP-I transitional entropies.

N^* phase in compound **4g**. Whilst compound **4a** is non-mesogenic, compound **4c** is enantiotropic nematogen with 24.2°C range. Upon lengthening the spacer by $n = 2$, the N^* temperature range is suppressed by almost 50% to only 12.2°C for compound **4e**. Further increase from $n = 9$ to $n = 11$ eventually results in the monotropic N^*

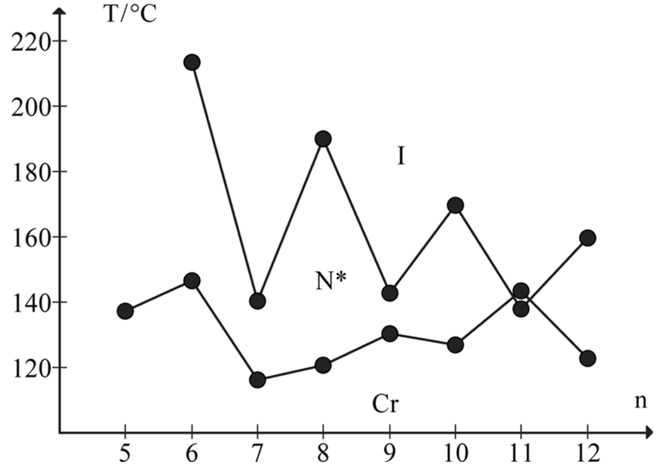

FIGURE 1 The dependence of the transition temperatures on the number of methylene units, n in the flexible spacers for compounds **4a**–**4h**.

phase for compound **4g**. The absence of nematogenic properties in compound **4a** is not immediately understood but it is presumably attributed to the insufficient flexibility due to the shorter spacer as compared to **4c** and **4e**, as well as the inclined conformation which reduces the molecular shape anisotropy.

The chiral nematic-isotropic transitional entropies of compounds **4b–4f** and **4h** are expressed in dimensionless quantity, $\Delta S_{N^*I}/R$ as listed in Table 1 whilst the dependence of these entropy values on *n* is illustrated in Fig. 2. An odd-even effect is observed of which the $\Delta S_{N^*I}/R$ values of the trimers with even-parity spacers are significantly higher than those recorded for the odd counterparts. For instance, the $\Delta S_{N^*I}/R$ value of compound **4d** ($\Delta S_{N^*I}/R = 4.53$) is ten times greater than the value for compound **4e** ($\Delta S_{N^*I}/R = 0.45$). The higher chiral nematic–isotropic entropy values for the even trimers as compared to the odd members are consistent with many other series of homologous liquid crystal oligomers regardless of whether the nematic phase is chiral or achiral. One such example is shown in a series of non-symmetric dimers which incorporates a cholesteryl moiety [13]. Due to the similarities in transitional properties between dimers and trimers, the pronounced difference in $\Delta S_{N^*I}/R$ magnitude between the even and odd trimers can, therefore, be reasonably justified based

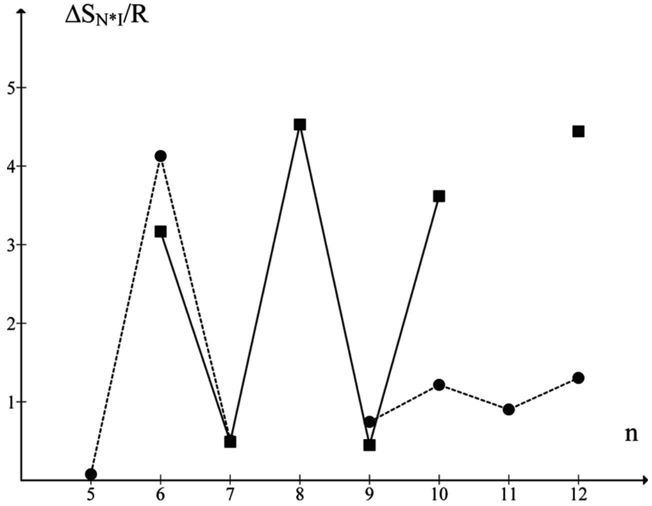

FIGURE 2 The dependence of chiral nematic–isotropic transitional entropy, $\Delta S_{N^*I}/R$ on the number of methylene units, *n* in the flexible spacers for compounds **4b–4f** and **4h**, and compounds **5a–5c** and **5e–5h** (dotted line) as previously reported [7].

on the understanding on the dimeric models. For even dimers, the higher nematic–isotropic transitional entropy is the result of greater structural compatibility with the molecular organization due to the linear molecular conformation [14]. However, it is important to mention that this point did not take into account the flexibility of the methylene spacers and hence, a more realistic explanation for the odd–even effect in nematic–isotropic transitional entropy should cover wider range of molecular conformation besides the presumed all-*trans* conformations. In the isotropic phase, it has been found that approximately half of the even-parity dimers are linear as opposed to only 10% of the counterparts with odd spacers are linear [14]. The synergy between conformational and orientational order therefore exists and at the transition to the nematic phase, many of these bent conformers are converted to the linear ones. Such transformation leads to greater orientational order of the nematic phase which subsequently results in higher nematic–isotropic entropy. For odd members, the difference in free energy between the bent and linear conformers is such that the orientational order of the nematic phase is insufficient for the bent-to-linear conversion [14]. Hence, the orientational order is not enhanced resulting in a smaller magnitude of the nematic–isotropic transitional entropy.

3.2. Optical Properties of Mesophases

For every homologue in the series except compound **4a**, the N^* phase is identified with the observation of oily streaks texture upon heating of the crystalline phase between two glass supports as shown in Fig. 3. The oily streaks are associated with planar anchoring of the director at the substrates, i.e., with the molecular long axis parallel to the glass plates which implies that the helical axis is perpendicular to these plates [15]. Upon cooling from the isotropic phase, instead of the oily streaks, the fan-shaped texture naturally predominates the entire domain. Contrary to oily streaks, the twist axis of the N^* fan-shaped texture deviates from the glass supports normal [15]. However, by shearing the sample mechanically during the cooling cycle, the oily streaks texture can be induced.

In addition to the N^* phase, compounds **4c** and **4e**, with respective heptyl and nonyl spacers, also exhibit the blue phase with platelet texture (Fig. 4). The blue phase temperature range is less than 1.0°C. Hence, in the DSC thermograms, the endothermic peak as well as the exothermic peak upon the cooling cycle involving N^*-BP-I transition and vice-versa appear unresolved. The DSC trace for compound **4c** is shown in Fig. 5. Under the microscopic light, the blue phase is

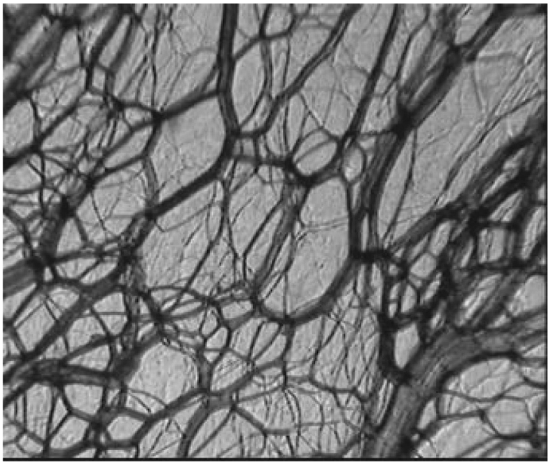

FIGURE 3 The N* oily streaks texture of compound **4b** at 170.1°C upon heating.

observed more apparently upon cooling the isotropic liquid rather than heating from the N* phase. The fact that the two odd-parity trimers exhibit the frustrated phase resembles characteristics which have been highlighted for several other odd oligomers including the (R)-2, 2′-bis{6-[4-(2-(2-fluoro-4-butyloxyphenyl)pyrimidine-5-yl)phenyloxy] alkyloxy}-1,1′-binaphthyls [16].

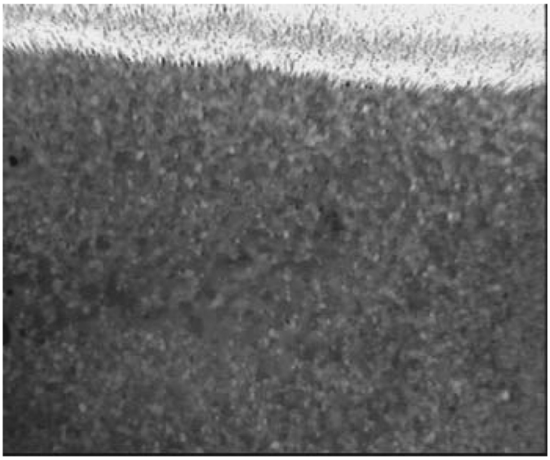

FIGURE 4 The photomicrograph showing the blue phase-N* transition upon cooling of compound **4c**.

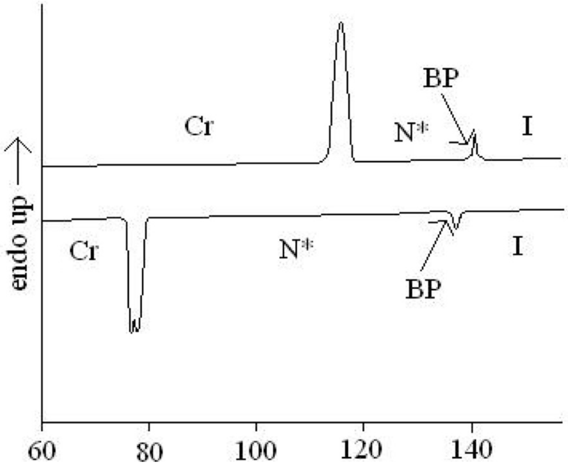

FIGURE 5 The DSC trace for compound **4c** with ±5°C min^{-1} heating and cooling rates.

3.3. Comparative Study between Compounds 4a–4h and Previously Reported 5a–5h

In order to study the influence of the presence of lateral bromine atoms on the liquid crystalline properties, comparison is made between the properties of compounds **4a–4h** and those of our earlier reported analogous trimers [7]. The trimers, with spacers ranging from pentyl to dodecyl, are labeled as **5a–5h** and the general molecular structure of the trimers is shown below.

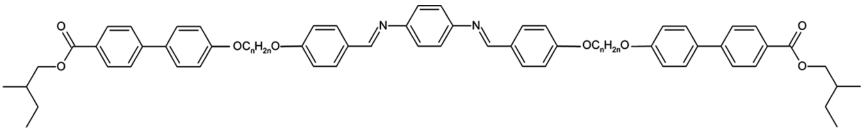

Compounds **5a–5h** exhibited various chiral mesophases. One of the distinctive differences that can be observed between the two series of trimers is that compounds **5a–5h** exhibited enantiotropic smectic phases, while **4a–4h** do not. Compound **5a**, for example, exhibited the ferroelectric SmC* and SmA phases for both heating and cooling cycles. On cooling, this trimer also exhibited an unidentified tilted smectic phase below the melting point. The smectogenic properties of compounds **5a–5h** indicate that the molecular breadth and shape anisotropy are important factors governing liquid crystallinity of the trimers. This point is further supported by the fact that the melting points and mesophase thermal stability of compounds **5a–5h** are significantly higher in comparison to those of compounds **4a–4h**. For example, the melting point of compound **4c** is 116.3°C, while the melting point for compound **5c** with similar heptyl spacer was 148.3°C, which is 32.0°C higher than that recorded for compound **4c**. The chiral nematic–isotropic transition temperatures are also higher for compounds **5a–5h** than for the title compounds, and interestingly, this difference is more pronounced for the odd members of the series (Fig. 6). This trend is similar to that reported for the homologous ether- and methylene-linked dimmers, although in our comparative study, the difference between compounds **4a–4h** and **5a–5h** is the presence of two lateral Br atoms in the former, and the absence of these atoms in the latter [17]. However, it is important to note that, despite these series of dimers and the present trimers having different chemical constitution for respective comparison, the underlying principle to explain the variation in the magnitude of nematic–isotropic transition temperatures is the same. For compounds **4a–4h**, the larger size of Br atom (atomic radius, 94 pm) as compared to H atom (53 pm) reduces the shape anisotropy of compounds **4a–4h** to an extent that the resulting effect is observed in the thermal properties of these compounds. In addition, the odd spacers in compounds **4a**, **4c**, **4e**, and **4g** cause the shape anisotropy of these compounds to decline further leading to

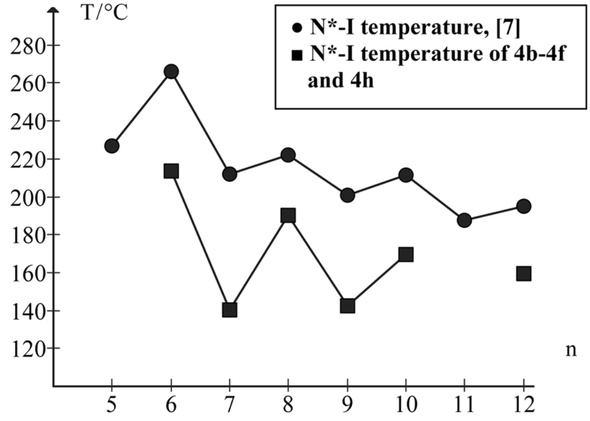

FIGURE 6 The comparison between N*-I transition temperatures of compounds **4b–4f**, **4h**, and those of the previously reported laterally unsubstituted analogous trimers [7].

the significantly lower chiral nematic-isotropic transition temperatures (Fig. 6). Although the Br atom induces higher polarizability in the molecules, this halogen atom is responsible for the increase of molecular breadth at the point of substitution due to its larger size, which consequently results in lower melting and clearing temperatures. A similar observation has also been recorded for chiral dimers which incorporate 4-(*trans*-4-*n*-hexylcyclohexyl)benzoic acid moiety with either a lateral fluorine or chlorine atom [18]. For compounds **4a–4h**, the lateral steric hindrance resulting from the presence of two Br atoms also explains the absence of smectogenic properties, despite the calamitic molecular geometry, which normally favors layered molecular arrangement.

Apart from the phase transition temperatures, the difference in transitional properties between the title compounds and the earlier reported compounds **5a–5h** can also be observed in terms of chiral nematic–isotropic transitional entropies especially those of the trimers with long spacers. In contrast to the $\Delta S_{N^*I}/R$ values of the title compounds, the values of the previously reported compounds **5a–5c** and **5e–5h** attenuate on increasing n, as shown in Fig. 2. As the result of the attenuation, the most pronounced difference, in terms of $\Delta S_{N^*I}/R$ values, between the two series is observed for compounds with $n = 10$ and 12. For compounds **5f** and **5h**, the $\Delta S_{N^*I}/R$ values are 1.21 and 1.31, while the values for the corresponding **4f** and **4h** are 3.62 and 4.44, respectively. As discussed, the $\Delta S_{N^*I}/R$ is associated with the orientational order of the nematic phase, taking into consideration the nature of molecular flexibility [14]. The higher values of $\Delta S_{N^*I}/R$ for compounds **4f** and **4h** suggest that the difference in free energy between the linear and bent conformations is smaller for these compounds than those for laterally unsubstituted compounds **5f** and **5h**, thus enabling the orientational order of the nematic phase to convert bent conformers into linear ones. Nevertheless, the higher $\Delta S_{N^*I}/R$ values of compounds **4f** and **4h** is still surprising, as it is not immediately clear how the presence of the relatively large Br atoms in the lateral position actually facilitates the conversion as opposed to compounds **5f** and **5h**. Such pronounced difference in the values of $\Delta S_{N^*I}/R$ between the trimers with comparable spacer length from the two series is apparently not observed for the members with $n = 6$ and 7. The respective $\Delta S_{N^*I}/R$ values for compounds **4b** and **5b** are 3.17 and 4.13, while for compounds **4c** ($\Delta S_{N^*I}/R = 0.49$) and **5c** ($\Delta S_{N^*I}/R = 0.51$), the values are almost the same. For both $n = 6$ and 7, the laterally unsubstituted trimers possess higher $\Delta S_{N^*I}/R$ values than the title compounds with lateral Br atoms.

4. CONCLUSIONS

Every chiral symmetric trimer 4,4′-bis{ω-[2-methylbutyl-4′-(4″-phenyl)-benzoateoxy]-3-bromo-4-alkyloxybenzylidene}-1,4-phenylenediamine in this series was mesogenic exhibiting the enantiotropic N* phase except members with pentyl and undecyl spacers. While the trimer with pentyl spacers is not mesogenic, the member with undecyl spacers exhibited the N* phase monotropically. The overall nematogenic properties and relatively lower transition temperatures of the trimers as compared to those of the earlier reported analogous trimers were associated with the increase of molecular breadth resulting from the presence of two lateral Br atoms at the *meta* position in the benzylidene-1,4-phenylenediamine core. The homologues with heptyl and nonyl spacers also exhibited the blue phase with platelet texture.

ACKNOWLEDGMENTS

The main author (G.-Y. Yeap) thanks the Ministry of Science, Technology, and Innovation (MOSTI) for the financial support through research grant no. 03-01-05-SF0366 (305/PKIMIA/613328). The authors also acknowledge Professor Ewa Gorecka (Warsaw University, Poland) and Professor Corrie T. Imrie (University of Aberdeen, Scotland) for suggestions and comments.

REFERENCES

[1] Imrie, C. T., & Henderson, P. A. (2002). *Cur. Op. Coll. Int. Sc.*, *7*, 298.

[2] Henderson, P. A., & Imrie, C. T. (2005). *Liq. Cryst.*, *32*, 1531.

[3] Tamba, M. G., Kosata, B., Pelz, K., Diele, S., Pelzl, G., Vakhovskaya, Z., Kresse, H., & Weissflog, W. (2006). *Soft Matter*, *2*, 60.

[4] Pal, S. K., Raghunathan, V. A., & Kumar, S. (2007). *Liq. Cryst.*, *34*, 135.

[5] Liao, C. C., Wang, C. S., Sheu, H. S., & Lai, C. K. (2008). *Tetrahedron*, *64*, 7977.

[6] Yoshizawa, A., Nakata, M., & Yamaguchi, A. (2006). *Liq. Cryst.*, *33*, 605.

[7] Yeap, G. Y., Hng, T. C., Mahmood, W. A. K., Gorecka, E., Takeuchi, D., & Osakada, K. (2009) *Mol. Cryst. Liq. Cryst.*, *506*, 109–133.

[8] Prajapati, A. K., Vora, R. A., & Pandya, H. M. (2001). *Mol. Cryst. Liq. Cryst.*, *369*, 37.

[9] Matharu, A. S., Cowling, S. J., & Wright, G. (2007). *Liq. Cryst.*, *34*, 489.

[10] Liao, Y. M., Janarthanan, N., Hsu, C. S., Gauza, S., & Wu, S. T. (2006). *Liq. Cryst.*, *33*, 1199.

[11] Kumar, S. (2003). *Pramana*, *61*, 199.

[12] Attard, G. S., Date, R. W., Imrie, C. T., Luckhurst, G. R., Roskilly, S. J., Seddon, J. M., & Taylor, L. (1994). *Liq. Cryst.*, *16*, 529.

[13] Marcelis, A. T. M., Koudijs, A., Karczmarzyk, Z., & Sudhölter, E. J. R. (2003). *Liq. Cryst.*, *30*, 1357.

[14] Imrie, C. T., & Luckhurst, G. R. (1998). *J. Mater. Chem.*, *8*, 1339.
[15] Dierking, I. (2003). *Textures of Liquid Crystals*, Wiley-VCH: Weinheim, Germany.
[16] Rokunohe, J., & Yoshizawa, A. (2005). *J. Mater. Chem.*, *15*, 275.
[17] Henderson, P. A., Niemeyer, O., & Imrie, C. T. (2001). *Liq. Cryst.*, *28*, 463.
[18] Yu, H., Huang, Z., Yin, B., Jamil, M., & Jeon, Y. J. (2008). *Mater. Lett.*, *62*, 3284.